JJMIE

Volume 1, Number 2, Dec. 2007
ISSN 1995-6665
Pages 69 - 77

Jordan Journal of Mechanical and Industrial Engineering

Effects of Condensate and Initial Formation of Thin Frost Layer on Evaporator Coil Performance of Room Air-Conditioners

Ahmed Hamza H. Ali *, Ibrahim M. Ismail

Department of Mechanical Engineering, Faculty of Engineering, Assiut University, Assiut 71516, Egypt.

Abstract

This study investigated experimentally and theoretically, how condensate and initial formation of a thin frost layer on the surface of the evaporator affects the evaporator performance of room air-conditioners compared to dry coil conditions. The theoretically obtained results were validated with the measured values in both wet and initial frost formation conditions and a good correlation was found. The results indicated that, at the same range of change in face velocity value, the total conductivity of a dry coil $(UA)_{dry}$ is increased by 38.8%. However, when it is combined with an increase in latent heat to the evaporator total cooling capacity ratio value (Q_{lat}/Q) of 10.6%, the total conductivity of wet coil $(UA)_{wet}$ is 45.4%. These results clearly indicate that the evaporator coil is characterized by higher performance under wet conditions compared to dry coil conditions. The results also show that the total conductivity after initial formation of a thin frost layer $(UA)_{Fr}$ has a higher value by about 8.2% than the dry coil condition. Moreover, the degradation in the evaporator coil performance under thin frost with a thickness up to one mm is only about 6.7%.

Keywords: Evaporator coil performance; Wet evaporator coil; Frosted evaporator coil; and Air dehumidifying;

Nomenclature

Alphabetic Symbols

A	: surface area, m^2
a'	: coefficient for fictitious enthalpy, J/kg
b'	: slope of i vs. T curve [31], J/kg K
c_p	: specific heat, J/kg K
d_o	: evaporator tube outer diameter, m
h	: heat transfer coefficient, W/m^2 K
i	: enthalpy, J/kg
k	: thermal conductivity, W/m K
L	: length, m
Le	: Lewis number, -
m	: fin perimeter, m^{-1}
$\dot{m}$	: mass flow rate, kg/s
q	: heat flux, W/m^2
Q	: total heat transfer rate, W
r	: radius, m
T	: temperature, K or ^oC
U	: overall heat transfer coefficient, $W/m^2.K$ or {$[W/m^2.K]/[J/kg]$}
V	: face velocity, m/s
W	: humidity ratio, $kg_{H2O}/kg_{dry\ air}$
x, y, z	: spatial co-ordinates, m

Greek symbols

ΔT_m	: logarithmic mean temperature difference, K
δ	: thickness, m
ϕ	: relative humidity
η	: fin efficiency, -

Subscripts

a	: air
avg	: average
c	: convection
cl	: cell
eff	: effective
eq	: equivalent
f	: saturated liquid
fin	: fin or fins
fr	: frost
g	: saturated vapor
I	: inner
in	: inlet
lat	: latent heat
m	: mean
o	: outer
out	: outlet
p	: pipe
r	: refrigerant

* Corresponding author. e-mail: ah-hamza@aun.edu.eg

s : saturation
sv : solid-vapor in sublimation
v : vapor
w : wet
wat : water
wb : wet-bulb

1. Introduction

The evaporator coils in air conditioning appliances provide the coldest surface for condensate formation from the air stream water vapor content in cooling operation mode as it cools and dehumidifies indoor air. As the amount of water condensed on the evaporator surface increases, water droplets are formed and intermittently drain due to gravity. Some water droplets adhere to the coil by surface tension phenomena. This is defined as hold-up condensate water. This hold-up water reacts with other indoor airborne contaminants and produces mold compounds and fouling resistance between the room air and the evaporator coil surface, Ali and Ismail [1]. Meanwhile, thin frost layer formation may occur on the evaporator surfaces of a room air-conditioner when it works as a heat pump in winter season. In this case, the outdoor air temperature is low and the evaporator operates at coil surface temperatures below 0^oC. It is found that some dust deposits on the outdoor heat exchanger of the air-conditioner, which sticks on the evaporator surface during the heating season with either condensate or an initial frost formation layer. Both compounds of water/dust depositions on the evaporator coil surface form a resistance to the heat transfer. Ali and Ismail [1] presented the effect of fouling deposits on room air-conditioner performance. In the literature, numerous studies have been conducted and provide detailed information relevant to both heat and mass transfer coefficients in the airside of fin and tube heat exchangers under dehumidifying conditions such as Yaun and Tucker [2], Jacobi et al. [3], Pirompugd et al. [4] and Halici and Taymaz [5]. Gravity-independent water separation within the condensing heat exchangers by the use of a hydrophilic fin surface coating, that promote the wetting and wicking of the condensate on the fin, were investigated by Shin et al. [6] and O'Neill et al. [7], while Lee et al. [8] investigated this effect in case of frost formation. Wetter [9] presented a simple simulation model of a dry finned water-to-air coil. Osada [10] reported that in the evaporator condensed water adheres to the fin surface and thus increases the pressure drop of the evaporator and degrades the heat transfer performance of the fins owing to louver blockage and water bridging. In addition, numerous studies have been conducted by using simulation models of thick frost layer formation and predicted the performance of fin and tube evaporator under these conditions such as [11 to 16]. The influence of thick frost formation on the performance of evaporator coils were investigated by either simulation or experimental studies by [17 to 23].

However, through a literature survey it was found that numerous experiments and models investigated the effect of water vapor condensate on the airside of evaporator surfaces mainly focused on the evaluation of both heat and mass transfer coefficients. Few examples cited that the condensate degrades the heat transfer performance of the evaporator coil fins as well as causes a decrease in the airflow area, thus leading to an increase of pressure drop through the evaporator coil. Ali and Ismail [1] found in their experiments that the clean wet-coil performance is higher than the dry-coil condition. Numerous studies investigated the influence of a thick frost formation layer on the evaporator coil, while the influence of initiation and thin frost layer formation on the evaporator coil performance is not clear. Thus, the performance of an evaporator coil of room air-conditioners, when its surface is covered by either condensate or initial frost layers without dust deposition on the coil, need to be clarified. Therefore, for room air-conditioners, this study aims at investigating experimentally and theoretically the effect of condensate and thin frost layer formation on the surface of evaporator coil on the performance of the evaporator coil compared to dry coil surface conditions. Experiments were carried out on a flat finned and staggered tube evaporator coil, while the theoretical model was used to clarify the effect of parameters on the evaporator coil performance which is difficult to measure experimentally.

2. Experimental Apparatus, Instrumentation and Procedure

2.1. Apparatus and Measurements

The test facility described in Ali and Ismail [1] is used to investigate the performance of the evaporator coil under wet and initial formation of thin frost layer conditions at various airflow rates with minor modifications in case of frost experiments. The modifications are: increasing the capillary tube length, and cooling the last 8 tubes in the condenser by water. A schematic diagram of the apparatus and its dimensions is shown in Figure 1.

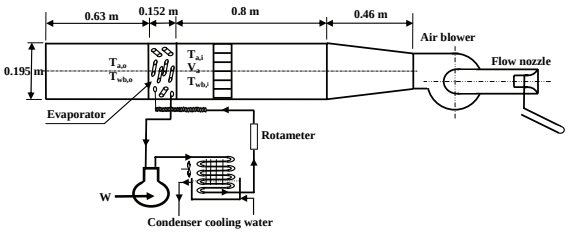

Figure 1: A schematic diagram of the test facility

The apparatus mainly consists of an air handling section, test section and the appropriately equipped instruments. The air handling sections include a nozzle meter, a variable speed airflow fan, an inlet air distribution plenum and a flow straightener (honeycomb). The flow straightener provides a uniform air velocity distribution at the inlet to the evaporator coil (test section). The evaporator coil frontal fined area dimensions are 0.254 x 0.191 m (10x7.5in) with a depth in flow direction of 0.152 m (6 in). It is a plate fin and tubes heat exchanger. The fins are made from aluminum alloy and the tubes are made from copper. Four rows of tubes with four tubes in depth are arranged in staggered manner ($2d_o$ x $2.5d_o$). The tubes are of 19.2 mm (3/4in) in outer diameter (d_o), fins pitch is fin/4.2mm (6 fin/in) and fin thickness is 0.6 mm. The test coil (evaporator) itself is a component of a compression refrigeration cycle using R12 as refrigerant, see Figure 1. The other main components of the refrigeration cycle include a hermetic compressor, an air-cooled condenser, a rotameter (uncertainty of ±0.01 l/min) for refrigerant mass flow measurements, 2 m long capillary tube for refrigerant

expansion, and 4 pressure gauges at inlet and outlet of both the evaporator and condenser with uncertainty of ±0.05 kPa. The input electric power to the compressor was measured by a Wattmeter with uncertainty of ±5W.

A variable electric resistor controlled the input power to the airflow fan motor. Thus, the airflow rate is controlled by the fan speed. The throat velocity of the air passing through the nozzle is determined by measuring the static pressure drop across the nozzle using water manometer with an accuracy of ±0.5 mm.

A data acquisition system having a resolution of 0.1°C is used to measure and record the temperatures. All temperatures are measured by using type T (copper/constantan) thermocouples with 0.5 mm diameter and an uncertainty of ±0.5 C. The thermocouples were used to measure the temperature at the following locations: 12 points air dry-bulb and wet-bulb temperatures before the evaporator coil, 6 points on the evaporator coil tubes and fins in addition, two points at refrigerant inlet and outlet, two points for ambient air dry-bulb and wet-bulb temperatures, respectively. The face air velocity at air inlet to the evaporator was measured using a portable digital anemometer with uncertainty of ±0.01 m/s.

2.2. Experimental Procedures and Data Reduction

To study the effect of dew formation on the performance, experiments were carried out in a quasi-steady state condition at different airflow rates corresponding to a face velocity ranging from 0.612 m/s to 5 m/s respectively. While for the case of initial formation of a thin frost layer, the face velocity was 0.612 m/s. This is because with this experimental apparatus and operating conditions, the frost is formed only at this low face velocity value. Stabilization of temperature readings to ± 0.1 °C in all thermocouple sensors was considered an indication of reaching a quasi-steady state condition, then the average of the temperature values are read and recorded. At the same time, the readings of the refrigeration cycle pressure gauges and rotameter as well as the manometer readings for the pressure difference across the nozzle were taken. The measurements were performed at the Heat Laboratory, Assiut University, Egypt. The experimental evaporator coil cooling capacity Q has been obtained from the energy balance on both refrigerant and air sides. It is given by:

$$Q=(Q_a+Q_r)/2 \qquad [W] \qquad (1)$$

where Q_a is the airside capacity of the evaporator coil. It is calculated by:

$$Q_a = \dot{m}_a(i_{a,1} - i_{a,2}) \qquad [W] \qquad (2)$$

where the air enthalpy, *i*, at the inlet and outlet of the evaporator coil is calculated by the formula of ASHRAE [24]. The air mass flow rate, $\dot{m}_a$, at the nozzle throat is calculated from the pressure drop across the nozzle. Q_r is the refrigerant side cooling capacity of the evaporator coil. It is calculated by:

$$Q_r = \dot{m}_r(i_{r,o} - i_{r,i}) \qquad [W] \qquad (3)$$

where the refrigerant enthalpy, *i*, at the inlet and outlet of the evaporator coil is obtained from [25] as a function of the temperature and pressure of state point. The refrigerant mass flow rate $\dot{m}_r$ is estimated from the rotameter reading and the refrigerant density. ASHRAE [24] relations were used to obtain the humid air properties ratio, W, at inlet and outlet of the evaporator coil from the measured data of air dry-bulb temperature, T_a, and air wet-bulb temperature, T_{wb}, respectively. The uncertainties were calculated through the data reduction of the experimental measurements based on the formula for computing overall errors of [26]; the uncertainty is estimated in determination Q ranging from 9.5% to 13.6%.

3. Thermal Model

The thermal model is used to investigate the factors influencing the evaporator coil performance, which are hardly to obtain by experimental measurements. These factors are the ratio of wet coil area to the total coil surface area, the ratio of the latent heat or sublimation heat capacities to the evaporator total cooling capacity and the effect of initial formation of thin frost layer thickness on the evaporator performance. The model is built for a flat fin air-to-refrigerant heat exchanger (evaporator coil) with staggered tubes shown in (Fig. 2-a). It is based on the discretization of the heat exchanger into cells. Each cell is one finned-tube in the refrigerant flow direction z as shown in Fig. (2-b).

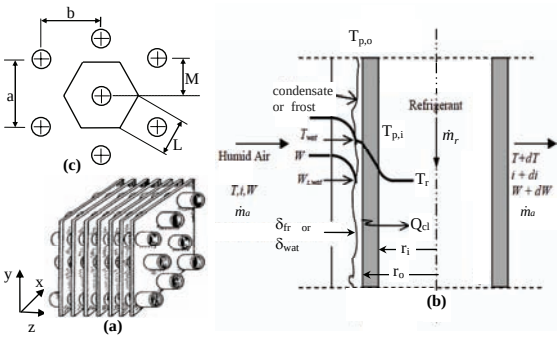

Figure 2: Schematic diagram of flat staggered fin-and tube evaporator coil with coordinate (a), energy and mass transfer balance on a cell (b) and hexagonal fin dimension parameters (c)

The refrigerant enters the evaporator as a two-phase mixture of saturated liquid and vapor with specific quality. Therefore, the energy variation is assumed to be one-dimensional in the flow direction and it is estimated from the enthalpy difference of the refrigerant between inlet and outlet from a cell. In contrast, the air dry-bulb temperature and its humidity ratio are varying in both x and y directions over each cell. Figure (2-b) shows a cell in the general case at which the surface could be dry, wet or with a thin frost layer at the cell surface. In the following subsections, modeling of the coil under these conditions is presented.

3.1. Dry Coil Surface Condition

For dry coil surface conditions, it is assumed that neither condensate nor frost is present on a cell surface shown in Fig. (2-b). The heat transfer rate for a cell, Q_{cl}, is obtained as follows: convection heat transfer from the air stream to the pipe outer surface and fins is sensible only and is calculated by:

$$Q_{cl} = h_{c,o}(A_{p,o} + \eta A_{fin})(T - T_{p,o}) \qquad [W] \qquad (4)$$

where $h_{c,o}$ is the outside convective heat transfer coefficient between air and dry surfaces of the cell. It is calculated from the correlation of a flat fin-and-tube heat exchanger of Wang [27]. $A_{p,o}$ and A_{fin} are the pipe outer surface areas and fin area in a cell, respectively. T is the air stream dry-bulb temperature, $T_{p,o}$ is the pipe outer surface temperature and η is the fin efficiency and is given by ASHRAE [24] in case of staggered tubes with continuous flat fins. In this study, η is treated as hexagonal fin as shown in Fig. (2-c) and given by:

$$\eta = \frac{\tanh(m r_o \varphi)}{m r_o \varphi} \qquad (5)$$

where

$$m = \sqrt{\frac{2h_{c,o}}{k_{fin}\delta_{fin}}},$$

$$\varphi = \left(\frac{r_{eq}}{r_o} - 1\right)\left[1 + 0.35\ln\left(\frac{r_{eq}}{r_o}\right)\right]$$

$$\frac{r_{eq}}{r_o} = 1.27\left(\frac{M}{r_o}\right)\left[\left(\frac{L}{M} - 0.3\right)\right]^{0.5}$$

where r_o is the inner radius of the fin, the pipe outer radius, see Fig. (2-b), r_{eq} is the equivalent radius of the fin, k_{fin} is the fin thermal conductivity, δ_{fin} is the fin thickness and a, b, L and M are dimension parameters as shown in Figure (2-c), respectively. The conduction through the pipe wall for one cell is given by:

$$Q_{cl} = \frac{2\pi L_p k_p (T_{p,o} - T_{p,i})}{\ln\left(r_o / r_i\right)} \qquad [W] \qquad (6)$$

where k_p, $T_{p,o}$ and $T_{p,i}$ are the pipe thermal conductivity, outer and inner surface temperatures, respectively. Convection from inner tube surface to the refrigerant for a cell is given by:

$$Q_{cl} = h_i A_{p,i}(T_{p,i} - T_r) \qquad [W] \qquad (7)$$

where h_i is the convective-evaporation heat transfer coefficient between the two-phase refrigerant and the inner surface of the pipe. It is a function of the two-phase refrigerant mass flow rate, refrigerant quality, pressure, temperature and internal pipe dimensions. Throughout the literature, only a few methods explained the details for calculating the local values of h_i such as [28] and [29]. In this study, the value of h_i is calculated by the techniques presented in Corberán [30]. T_r is the refrigerant temperature. From Eqs. (4), (6) and (7) the value of Q_{cl} can be also expressed by:

$$Q_{cl} = U_o A_o \Delta T_m \qquad [W] \qquad (8)$$

where U_o is given by:

$$U_o = \frac{1}{\frac{A_o}{A_{P,i}h_i} + \frac{A_o \ln\left(r_o / r_i\right)}{2\pi k_p L_p} + \frac{A_o}{\eta A_{fin} h_{c,o}} + \frac{A_o}{A_{P,o}h_{c,o}}}$$

$$[W/m^2.K] \qquad (9)$$

The logarithmic mean temperature difference, ΔT_m, between the air stream and refrigerant with the probability of refrigerant superheating at the outlet from the pipe at the last cell is given by:

$$\Delta T_m = \frac{(T_{a,in} - T_{r,out}) - (T_{a,out} - T_{r,in})}{ln\left[\frac{(T_{a,in} - T_{r,out})}{(T_{a,out} - T_{r,in})}\right]} \qquad [K] \qquad (10)$$

3.2. Wet Coil Surface Condition

As the moist air is cooled and its temperature decreases below the water vapor dew point temperature, the water vapor condenses on the evaporator coil surface. For wet coil conditions, both the heat transfer and mass transfer between the moist air and a thin condensate film takes place simultaneously according to the enthalpy difference as cited in [31]. In this part of the model the following assumption are used: the outer surface of fins and tubes are covered with a thin water film, the boundary layer of saturated moist air is at the thin water film temperature, which is equal to both the tube and modified fins surface temperature. The equation for convection heat and mass transfer between humid air and wet cell surfaces, shown in Fig. (2-b), is given by [31] as follows:

$$Q_{cl} = \frac{h_{c,o}A_o}{c_{p_a}}\left[(i - i_{s,wat}) + \frac{(W - W_{s,wat})(i_{g,T} - i_{f,wat} - i_g^0 Le)}{Le}\right]$$

$$[W] \qquad (11)$$

with total outer surface area of the cell A_o, enthalpy i, humidity ratio W, specific heat c_p and Lewis number Le. To consider the conduction across the water film thickness shown in Fig. (2-b), conduction through the pipe wall and internal convection evaporation between the refrigerant and inner pipe surface Q_{cl} value is calculated by;

$$Q_{cl} = U_{o,w} A_o \Delta i_m \qquad [W] \qquad (12)$$

where $U_{o,w}$ is the overall heat transfer coefficient in wet condition based on the enthalpy potential. It is given by:

$$U_{o,w} = \frac{1}{\frac{b'_r A_o}{A_{p,i}h_i} + \frac{b'_p A_o \ln\left(r_o / r_i\right)}{2\pi k_p L_p} + \frac{b'_{wat} A_o}{A_{fin}\eta_w h_{o,w}} + \frac{b'_{wat} A_o}{A_{p,o}h_{o,w}}}$$

$$[(W/m2)/(J/kg)] \qquad (13)$$

where $b_r^{'} = \frac{i_{s,p} - i_{s,r}}{T_p - T_r}$, $i_{s,p}$ and $i_{s,r}$ are fictitious enthalpies of saturated moist air valuated at the pipe and refrigerant temperatures, respectively. The value of $i_{s,p}$ is defined in [31] by $i_{s,p} = a_{wat}^{'} + b_{wat}^{'} T_p$, where $a^{'}$ and $b^{'}$ are coefficients to be calculated from plots in [31] at the air saturation condition corresponding to the pipe temperature. Similarly the values of $i_{s,r}$, $b_p^{'}$ and $b_{wat}^{'}$ can be calculated, respectively. The wet fin efficiency, η_w, is calculated at $h_{o,w}$. The combined convection and evaporation heat transfer coefficient, $h_{o,w}$, between moist air and outer cell surfaces area is calculated by:

$$h_{o,w} = \frac{1}{\frac{cp_a}{b_{wat}^{'} h_{c,o}} + \frac{\delta_{wat}}{k_{wat}}} \qquad [W/m^2.K] \qquad (14)$$

Δi_m value is calculated by:

$$\Delta i_m = \frac{(i_1 - i_{s,r,2}) - (i_2 - i_{s,r,1})}{ln\frac{(i_1 - i_{s,r,2})}{(i_2 - i_{s,r,1})}} \qquad [J/kg]$$

where i_1 and i_2 are enthalpies of the entering and leaving air stream of a cell, $i_{s,r,1}$ and $i_{s,r,2}$ are fictitious enthalpies of saturated air calculated at entering and leaving refrigerant temperatures of a cell and are estimated as defined in [31] . The pipe inner surface temperature is calculated from:

$$T_{p,i} = T_r + \frac{Q_{cl}}{h_i A_{p,i}} \qquad [K] \qquad (15)$$

The total heat transferred from the air stream to the cell surface consists of two parts: the sensible part and the latent part. Using the relation of convective heat and convective mass transfer by Le number relation, the outer pipe surface temperature is compared with the inlet air dew point temperature to the cell in order to clarify at which cell the condensate begins. It is calculated by:

$$Q_{cl} = h_{c,o}\left[1 + \frac{(W - W_{s,p})\ i_{fg}}{Le\ \ c_{p_a}(T - T_{p,o})}\right](T - T_{p,o})(A_{p,o} + \eta A_{fin}) \qquad [W] \qquad (16)$$

where i_{fg} is the enthalpy for latent heat of condensation.

3.3. Frost Coil Surface Condition

In this part of the model, a correlation that considers the molecular diffusion of water vapor inside an initially formed frost layer, mass and heat transfer between air stream and frosted coil surface is used to predict the effect of an initial formation of a thin frost layer on the evaporator coil surface and the thin frost thickness effect on the evaporator performance. The following assumptions are considered: all heat and mass transfer surfaces are covered with thin frost layer and this layer is to be characterized by average properties; frost thermal conductivity varies only with frost density.

The total heat transfer rate in a cell with frosted surface conditions is calculated by:

$$Q_{cl} = U_{o,fr} A_o \Delta T_m \qquad [W] \qquad (17)$$

where $U_{o,fr}$ is given by:

$$U_{o,fr} = \frac{1}{\frac{A_o}{A_{P,i} h_i} + \frac{A_o\, ln\left(r_o / r_i\right)}{2\pi k_p L_p} + \frac{\delta_{fr}}{k_{fr}} + \frac{A_o}{\eta A_{fin} h_{eff}} + \frac{A_o}{A_{P,o} h_{eff}}} \qquad [W/m^2.K] \qquad (18)$$

k_{fr} and δ_{fr} are the frost thermal conductivity and thickness, respectively. The equations presented in [19] for k_{fr} and δ_{fr} are used in this study. h_{eff} is effective combined sensible/ sublimation heat transfer coefficient. By similarity with eq. (16) it is calculated by:

$$h_{eff} = h_{c,o}\left[1 + \frac{(W - W_{s,fr})\ i_{sv}}{Le\ \ c_{p_a}(T - T_{fr,o})}\right] \qquad [W/m^2.K] \qquad (19)$$

where i_{sv} is the enthalpy for heat of sublimation and $T_{fr,o}$ is the frost layer surface temperature which is calculated by:

$$T_{fr} = \frac{Q_{cl}}{h_{eff} A_o} - T \qquad [K] \qquad (20)$$

3.4. Solution Techniques

The inlet conditions for both the air and refrigerant are input into the model. The solution method of the equation in general is based on an iterative solution procedure for pipe temperatures. First, a guess is made for pipe temperature distribution in each cell, and then the governing equations for the refrigerant are solved in an explicit manner. Once the refrigerant properties are obtained for any fluid cell, the pipe temperatures at every pipe cell are estimated from the heat transferred across it. This procedure is repeated until convergence is reached. In the airside, depending on the operating condition parameters, some cells may operate with a dry surface, and with remainder of its wet surface. Detailed procedures for the solution of humid air are in ARI [32] and can be summarized as follows: the evaporator is first treated as dry, then the inlet dew point temperature of the air is compared with the wall temperature of cells. From the heat transfer rate equation the outlet enthalpy is calculated, and then the outlet air temperature. At cells where the pipe wall temperature is equal to the inlet air dew point temperature of the cell, the calculation for a wet coil is integrated. Then, the latent heat portion is calculated as the difference between the total heat and the sensible heat. From the latent heat portion, the outlet humidity values from the cells are calculated. The evaporator coil

dimensions described in the experimental section with the aid of the equations for calculation of A_o and A_{fin}, which are given in ARI [32], are input into the model. The mean hold-up water thickness, δ_{wat} , remaining on the evaporator surfaces and the frost thickness δ_{fr} are set to 0.1 mm in case of investigating other parameters than their thickness. The Lewis number (Le) is set to 1. A computer program based on this model was written in FORTRAN language. In the program, air properties are calculated with using ASHRAE [24] equations and refrigerant properties are calculated by using subroutine PROPERTY of ASHRAE [25].

4. Results and Discussion

4.1. Effect of Condensate on Evaporator Coil Performance

The results presented in this study are based on a quasi-steady state condition. Among many measurements that were carried out for face velocities ranging from 0.612 m/s to 5 m/s, it was observed experimentally that there is no condensate for experiments performed at face velocities greater than 1 m/s. Therefore, there was a significant contact time required between moist air and the evaporator coil surface for dew formation. In addition to this factor, the lower air relative humidity as seen from Figure (3-a) inside the laboratory during the experiments time, is anther factor contributing to this effect. However, in order to investigate the effect of condensate formation on the evaporator coil performance, all experiments were carried out with inlet refrigerant temperature higher than 0 °C, to avoid frost formation on the coil surface. The measured values of variation of inlet air dry-bulb temperature entering the evaporator coil, refrigerant inlet temperature to evaporator coil as well as the determined air water continent humidity ratio and relative humidity both were calculated from the measured wet-bulb and dry-bulb temperatures at various air face velocity as shown in Figure (3-a). The calculated values of outlet air dry-bulb temperature, air water continent humidity ratio and the evaporator coil total cooling capacity, from the input operating conditions data to the model that is shown in Figure (3-a), are compared with their corresponding experimentally determined values as shown in Figures (3-b,c and d), respectively. As seen from the Figure (3), the model of wet coil condition predicts the performance of the evaporator coil within 10% of relative error without any specific adjustment. Thus, it can be considered that a good agreement was obtained as the calculated values lay within the range of experimental uncertainty. This agreement validates the calculated results of the evaporator coil performance under condensate formation.

The model is used to investigate the characteristic parameters to clarify the effect of dew formation on the evaporator coil performance. The obtained results from the wet coil model are shown in Figure (4). These results were obtained with the input operating conditions shown in Figure (3-a). Comparing the total conductivity (UA) values in both wet and dry conditions, their values presented in Figure (4-a) are based on logarithmic mean temperature difference of Eq. (10). As stated previously, in the presented range of face velocity, drainage of condensate from the evaporator coil is observed experimentally, until a face velocity value of 1m/s.

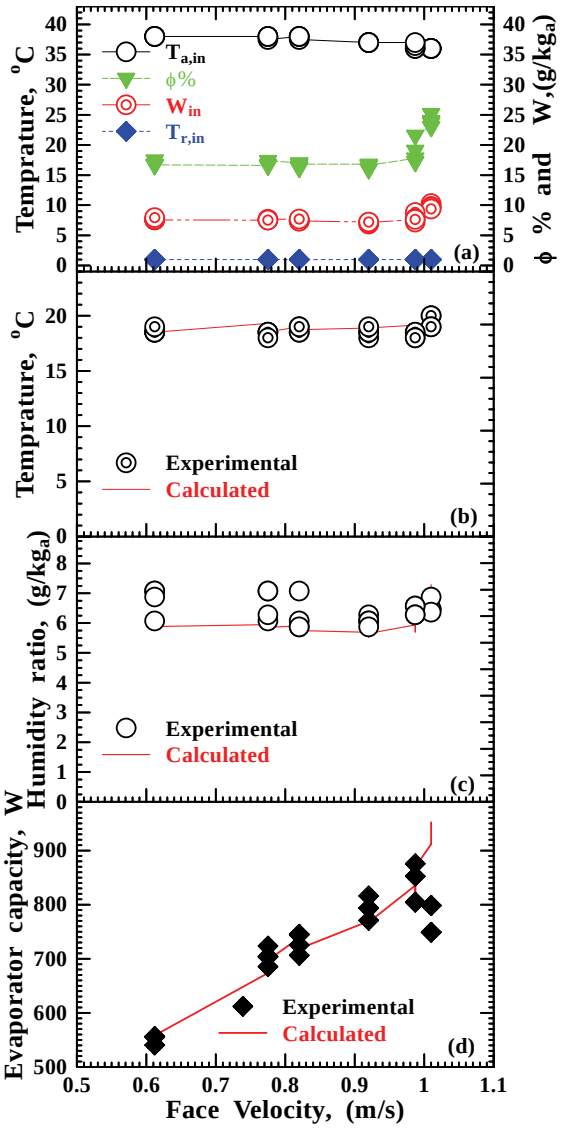

Figure 3: Measured entering operating conditions to the evaporator coil at wet condition (a), comparison of the calculated values with correspondence measured values, outlet air dry-bulb temperature (b), outlet air humidity ratio, (c) and evaporator cooling capacity (d)

In this range of face velocity, this observation agrees with the model results of 100% wet coil surface that are shown in Figure (4-b). From Figure (4-a), it is clear that both calculated (UA) values, for dry and wet conditions increases with increase in the face velocity values. This result is expected because the heat transfer coefficient is dependant on the flow Reynolds number, in which it is a function of the face velocity. While, the value of (UA) in wet conditions is higher than the case of dry coil and the difference between both (UA) values increases as the latent heat ratio value increases. This can be attributed to the following: in the present experiments, the fin pitch is 4.23mm, the retained condensate droplets on the coil do not bridge the inter-fin gap but increase the heat transfer rate. The higher $(UA)_{wet}$ value instead of retained condensate thin layer, which can represent conduction resistance, can be explained with aid of group in the

brackets of Eq. (16). The term in the bracket is the dry convective heat transfer coefficient plus the portion of latent heat of condensation.

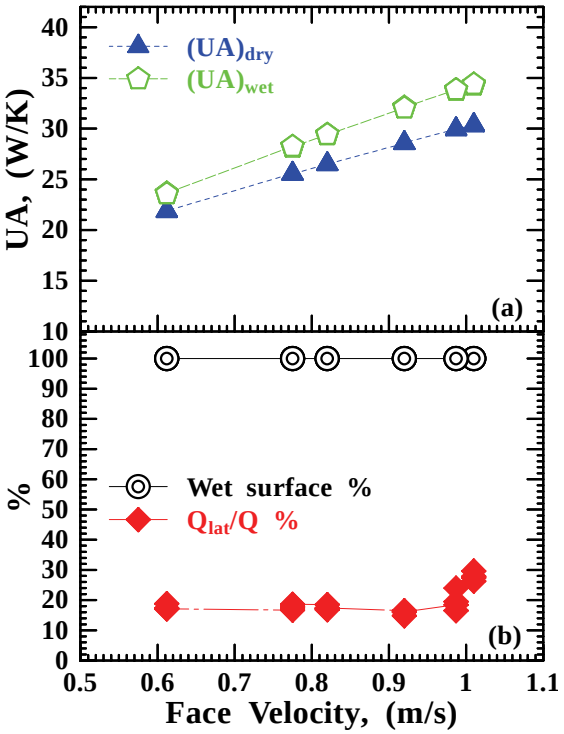

Figure 4: Characteristics of the evaporator coil under wet condition

The increase in $(UA)_{wet}$ value is function of inlet air dry-bulb temperature and humidity ratio and refrigerant temperature, with considering the conduction resistance in the tube wall is very small. The ratio of the increase on $(UA)_{wet}$ value can be clearly explained in quantity values as follows: at the latent heat to the evaporator total cooling capacity ratio (Q_{lat}/Q) value of 18.2% the values of (UA) in both dry and wet coil were 21.85 and 23.6 (W/K), respectively. While, at (Q_{lat}/Q) value of 29.64%, UA values became 30.32 and 34.31 (W/K), respectively. Thus, for the same range of a change in face velocity value, $(UA)_{dry}$ is increased by 38.76%, while when it is combined with an increase in (Q_{lat}/Q) value by 10.64%, the $(UA)_{wet}$ is 45.4%. These results clearly indicate that, an evaporator coil with higher fin-pitch is characterized by higher performance under wet condition than the dry coil surface condition and the retained condensate has an important effect on the evaporator coil performance enhancement.

4.2. Effect of Initial Formation of Thin Frost Layer on the Evaporator Coil Performance

To investigate the effect of initial formation of thin frost layer on the evaporator coil, the experimental apparatus had a minor modification compared to that described before in order to obtain entering refrigerant temperature less than 0°C. With this modification, initial formation of thin frost layer on the coil is built at low face velocity values only. An experiment was carried out for number of hours with thin frost layer formed on the evaporator coil. The measured entering conditions to the coil are shown in Fig. (5-a). The model results for the outlet air humidity ratio under frost condition were compared with experimentally obtained value as shown in Figure (5-b). It can be seen from Figure (5-b) that both results are in good agreement with the scale measurements (±7%). The calculated (UA) values for both dry and frosted coil conditions as well as the sublimated heat to the evaporator total cooling capacity ratio (Q_{sv}/Q) values are shown in (5-c). As shown in Figure (5-c), (UA) values are constant with time variation in both coil conditions instead of change in (Q_{sv}/Q) values. Also, the results shown in the figure indicate that the total conductivity under initial formation of thin frost layer $(UA)_{fr}$ has higher values than dry coil condition, for the presented operating conditions, by about 8.2%. The higher value of $(UA)_{fr}$, instead of the thin frost layer that added conduction resistance to heat transfer, can be explained with the aid of the brackets in Eq. (19). The value in the brackets is the sum of dry convective heat transfer coefficient plus the sublimated heat portion ratio.

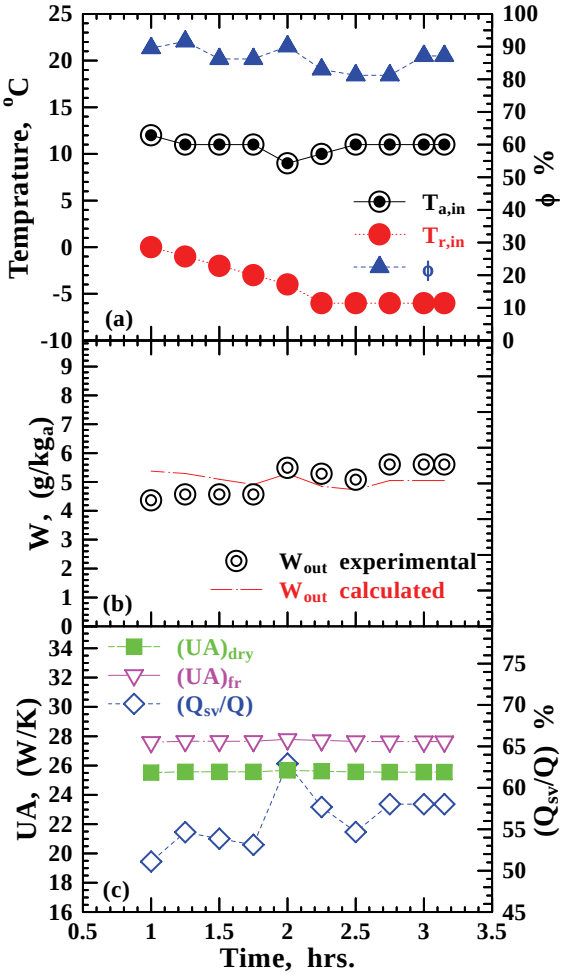

Figure 5: Measured entering operating conditions to the evaporator coil at frost condition (a), the calculated outlet air humidity ratio under frost condition compared with correspondence experimental one (b) and characteristics of the evaporator coil under thin frost formed layer (c)

Interpretation of this results are based on morphology diagram presented in Libbrecht [33], in which the initial frost layer, at tube temperature range of 0 to -5°C, consists

of a porous structure composed of individual ice crystals and air pockets. Based on this physical structure, the initial frost formation provide more pores for diffusion of the difference of air moister content ($W-W_{s,fr}$) into this initial frost layer. This difference in the air humidity is converted into frost and combined by extraction to the sublimation heat from the air stream, which has a positive effect on the heat transfer rate between the air stream and the coil. These results clearly indicate that, the evaporator coil surface with higher fin-pitch has higher performance under initial formation of thin frost layer compared with dry coil surface condition.

4.3. Effect of Frost Thin Thickness on the Evaporator Coil Performance

In the experiments for investigation of the effect of frost formation on the coil performance, no instruments were used to measure the frost thickness due to the difficulty in measuring the frost thickness in a full-scale evaporator coil. Therefore, the model is used to investigate the effect of thin formed frost thickness layer on the coil surface up to one mm on the evaporator coil performance. The result is presented in the form of the total conductivity under frost condition $(UA)_{fr}$. The calculated result correspondence to the operating conditions of face velocity equal 0.612 m/s, entering air dry-bulb temperature of 10°C, inlet air relative humidity of 87.1% and inlet refrigerant temperature of -6 °C is presented in Figure (6).

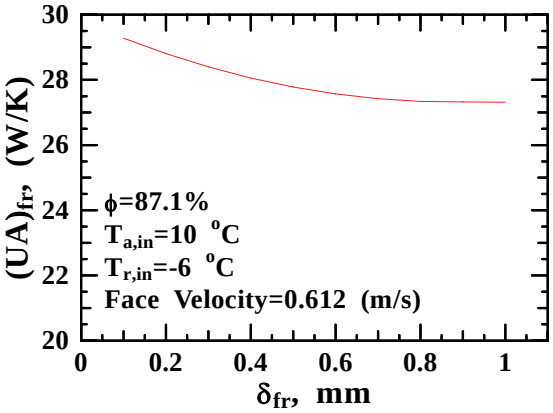

Figure 6: Effect of initial thin frost layer on the evaporator coil total conductivity (UA)fr

The result indicates that the degradation in $(UA)_{fr}$ value for frost layer thickness up to one mm is only about 6.7%. Explanation of this result is as stated in the previous subsection. Thus, it can be concluded that, the reduction in coil total heat transfer rate due to initial thin frost layer up to one mm at the stated operating condition has insignificant effect on the evaporator coil performance. While, through the aforementioned literature concerning the degradation on the evaporator coil performance at deep freezing temperatures under frost condition may be explained by the fact that, frost formation on heat exchanger surface at these low temperature has different construction, non-pours, as shown in morphology diagram presented in [33]. In addition, greater frost thickness with low fin-pitch leads to blocking of the airflow paths followed by a greater reduction of airflow rate and higher-pressure drop through the evaporator coil, resulting in a greater reduction of the evaporator coil performance. In addition, it causes additional thermal conduction resistance on the coil surface leading to dramatic decreases in the evaporator coil performance.

5. Conclusions

This study investigated experimentally and theoretically the effects of condensate and initial formation of thin frost layer on the evaporator coil surface on the performance of the evaporator coil of room air-conditioners compared with dry coil surface conditions. Experiments were carried on flat fin and staggered tube evaporator coil, while the theoretical model was used to clarify the effects of parameters which are difficult to measure in the experiments on the evaporator coil performance. The obtained results are summarized as follows:

- The model results were validated with the measured data in both wet and initial frost formation conditions of the evaporator coil, and the predicted results are within 10 % of relative error. This validation is considered a good agreement as the calculated values are within the range of experimental uncertainty.
- For the same range of a change in face velocity value, $(UA)_{dry}$ is increased by 38.76%, while when it is combined by an increase in (Q_{lat}/Q) value by 10.64%, the $(UA)_{wet}$ is 45.4%.
- The evaporator coil with higher fin-pitch is characterized by higher performance under wet condition than the dry coil surface condition.
- The total conductivity under initial formation of thin frost layer $(UA)_{fr}$ has higher values than dry coil condition by about 8.2% in the range of operating conditions of this study.
- At the stated operating condition, the degradation in $(UA)_{fr}$ under thin frost thickness up to one mm is only about 6.7% that has insignificant effect on the evaporator coil performance.

References

[1] Ali, Ahmed Hamza H. and Ismail, Ibrahim M, “Effect of the evaporator airside fouling on performance of room air conditioners and its impact on indoor air quality”, ASHRAE Int. J. of HVAC&R Research, 2007, Accepted for publication

[2] Yaun Y. H. and Tucker A. S., “The performance study of a wet six-row heat-pipe heat exchanger operating in tropical buildings”. Int. J. Energy Res., Vol. 27, 2003, 187–202.

[3] Jacobi A. M., Park Y., Zhong Y., Michna G., and Xia Y., “High Performance Heat Exchangers for Air-Conditioning and Refrigeration Applications (Non-Circular Tubes)”. ARTI-21CR/605-20021-01, Final Report, July 2005

[4] Pirompugd W., Wongwises S. and Wang C., “Simultaneous heat and mass transfer characteristics for wavy fin-and-tube heat exchangers under dehumidifying conditions”. Int. J. of Heat and Mass Transfer, Vol.49, 2006, 132–143.

[5] Halici F. and Taymaz I., “Experimental study of the airside performance of tube row spacing in finned tube heat exchangers”. Heat Mass Transfer, Vol. 42, 2006, 817-822.

[6] Shin J. and Ha. S., "The effect of hydrophilicity on condensation over various types of fin-and-tube heat exchangers". Int. J. of Refrigeration Vol. 25, 2002, 688-694.
[7] O'Neill C., Beving D.E., Chen W. and Yan Y., "Durability of hydrophilic and antimicrobial zeolite coatings under water immersion". AIChE J., Vol. 52, No. 3, 2006, 1157-1161.
[8] Lee H., Shin J., Ha S., Choi B. and Lee J., "Frost formation on a plate with different surface hydrophilicity". Int. J. of Heat and Mass Transfer Vol. 47, 2004, 4881-489.
[9] Wetter M., "Simulation Model Finned Water-to-Air Coil without Condensation". Lawrence Berkeley National Laboratory Report LBNL-42355, January 1999.
[10] Osada H., Aoki H., Ohara T. and Kuroyanagi I., "Research on corrugated multi-louvered fins under dehumidification". Heat Transfer Asian Research, Vol. 30, No. 5, 2001, 383-393.
[11] Hong C. H., "Modeling and measurement of frost characteristics on heat exchanger surfaces". PhD. Thesis, University of Saskatchewan, Saskatoon, Canada, 2000.
[12] Watters R. J., O'Neal D. L. and Yang J., "Evaluation of Fin Staging Methods for Minimizing Coil Frost Accumulation". ASHRAE Res. Project: 1002-RP, July 2000.
[13] Yang J., "A study of heat pump fin staged evaporators under frosting conditions". PhD Dissertation, Texas A&M University, 2003.
[14] Chen H., Thomas L. and Besant R. W., "Fan supplied heat exchanger fin performance under frosting conditions". Int. J. of Refrigeration Vol. 26, 2003, 140-149.
[15] Hoffenbecker N., "Investigation of Alternative Defrost Strategies". M. Sc Thesis University of Wisconsin-Madison, 2004.
[16] Liu Z., Zhu H. and Wang H., "Study on transient distributed model of frost on heat pump evaporator". J. of Asian Architecture and Building Engineering, Vol. 4, No. 1, 2005, 265-270.
[17] Horuz I., Kurem E. and Yamankaradeniz R., "Experimental and theoretical performance analysis of air-cooled plate-finned-tube evaporators". Int. Comm. Heat Mass Transfer, Vol. 25, No. 6, 1998, 787-798.
[18] Verma P., Carlson D. M., Wu Y., Hrnjak P. S. and Bullard C. W., "Experimentally validated model for frosting of plain-fin-round-tube heat exchangers". Proc. of IIF–IIR Commission D1/B1 – Urbana, IL, 2002.
[19] Seker D., Karatas H., Egrican N., "Frost formation on fin-and-tube heat exchangers. Part I-Modeling of frost formation on fin-and-tube heat exchangers". Int. J. of Refrigeration, Vol. 27, 2004, 367–374.
[20] Seker D., Karatas H., Egrican N., "Frost formation on fin-and- tube heat exchangers. Part II-Experimental investigation of frost formation on fin-and-tube heat exchangers". Int. J. of Refrigeration, Vol. 27, 2004, 375–377.
[21] Aljuwayhel N. F., "Numerical and Experimental Study of the Influence of Frost Formation and Defrosting on the Performance of Industrial Evaporator Coils". PhD Dissertation, University of Wisconsin-Madison, 2006
[22] Muehlbauer, J., "Investigation of Performance Degradation of Evaporator for Low Temperature Refrigeration Applications". M. Sc Thesis, University of Maryland, College Park, 2006.
[23] Yao Y., Jiang Y., Deng S. and Ma Z., "A study on the performance of the airside heat exchanger under frosting in an air source heat pump water heater/chiller unit". Int. J. of Heat and Mass Transfer, Vol. 47, 2004, 3745-3756.
[24] ASHRAE (2005). 2005 Fundamentals Handbook SI. American Society of Heating, Refrigerating and Air-Conditioning Engineers. Atlanta, Georgia.
[25] ASHRAE, HVAC1 Toolkit: A Toolkit for Primary HVAC System Energy Calculations. American Society of Heating, Refrigerating and Air-Conditioning Engineers. Atlanta, Georgia, 1999.
[26] Doeblin, E. O. Measurement Systems, Application and Design. McGraw-Hill Book Co; 1990.
[27] Wang, C.C., Chi, K.Y., and Chang, C.J., "Heat transfer and friction characteristics of plain fin-and-tube heat exchangers, part II: correlation". Int. J. of Heat Mass Transfer, Vol. 43, 2000, 2693-2700.
[28] Payne, W. V. and Domanski, P. A., "Potential Benefits of Smart Refrigerant Distributors. ARTI-21CR/610-20050-01, Final Report, January 2003.
[29] Corberán J. M., Fernández de Córdoba P., Ortuño S., Ferri V., Setaro T. and Boccardi J., "Modeling of tube and fin coils working as evaporators or condensers". Proc. of third European Thermal Sciences Conf., Heidelberg, Germany, 2000.
[30] Corberán, J. M., Fernández de Córdoba, P., Ortuño S., Ferri, V., Gonzálvez, J., Setaro T. and Boccardi J., "Modelling of compact evaporators and condensers". Proc. of Sixth Int. Conf. on Advanced Computational Methods in Heat Transfer, Madrid, 2000.
[31] Kuehn T. H., Ramsey J. W. and Threlkeld J. L. Thermal Environmental Engineering 3rd Ed., Prentice Hall; 1998.
[32] ARI Standard 410-2001 with Addendum 2, Forced-Circulation Air-Heating and Air-Cooling Coils. May 2005.
[33] Libbrecht, K. G., "The physics of snow crystals". Institute of Physics Publishing, Reports on Progress in Physics, Vol. 68, 2005, 855–895.